Marine Pollution Bulletin

Nanoplastics and ocean warming: combined impact on physiology and surface properties of the marine microalga Dunaliella tertiolecta

--Manuscript Draft--

Manuscript Number:	
Article Type:	Research Paper
Keywords:	microalga Dunaliella tertiolecta; nanoplastics; ocean warming; oxidative stress biomarkers; photosynthetic performance; cell nanomechanical properties
Corresponding Author:	Tea Misic Radic, Ph.D. Ruđer Bošković Institute Zagreb, Zagreb CROATIA
First Author:	Petra Vukosav, PhD
Order of Authors:	Petra Vukosav, PhD
	Bruno Komazec, PhD
	Petra Peharec Štefanić, PhD
	Darija Domazet Jurašin, PhD
	Tea Misic Radic, Ph.D.
Abstract:	Ocean warming due to climate change, in combination with emerging pollutants such as nanoplastics, poses a growing threat to marine ecosystems. This study investigates the combined impact of amine-modified polystyrene nanoplastics (PS-NH_2 NPs, diameter 51 nm) and elevated temperature (30 °C) on the physiology and surface properties of the marine green microalga Dunaliella tertiolecta. We assessed responses at both single-cell and population levels by examining growth dynamics, reactive oxygen species (ROS) production, oxidative stress biomarkers, photosynthetic efficiency and changes in nanostructural and nanomechanical cell properties. Short-term exposure (5 days) to PS-NH_2 NPs significantly inhibited algal growth at both 18 °C and 30 °C, with stronger inhibition and lower EC_{50} values at 30 °C. Nanoplastics induced excessive ROS production at both temperatures, leading to increased lipid peroxidation and increased activities of antioxidant enzymes. Photosynthetic performance decreased significantly at both temperatures as reflected by a lower maximum quantum yield of PSII (Fv/Fm) and a lower performance index (PIabs). While the nanoplastics adhered to the surface of the algal cells at both temperatures, the effects on nanomechanical properties were temperature dependent. At 18°C, the PS-NH_2 NPs had a negligible effect on cell stiffness and adhesion. However, simultaneous exposure to nanoplastics and elevated temperature significantly reduced both cell stiffness and adhesion, suggesting that heat stress enhances the adverse effect of nanoplastics on cell surface integrity. Overall, this study highlights how nanoplastics and ocean warming synergistically impact microalgae and provides new insights into the ecological risks posed to marine microalgae under future climate scenarios.

Cover Letter

Dr. Tea Mišić Radić
Senior research associate
Ruđer Bošković Institute, Division for Marine and Environmental Research
Bijenička 54, 10000 Zagreb, Croatia
tmisic@irb.hr

Editors-in-Chief: **Prof. Dr. Michel Boufadel**
Prof. Dr. Francois Galgani
Prof. Dr. Gui-Peng Yang

Marine Pollution Bulletin

16 July 2025

Dear Editors **Prof. Dr. Michel Boufadel, Prof. Dr. Francois Galgani and Prof. Dr. Gui-Peng Yang,**

We are pleased to submit our original research article entitled "***Nanoplastics and ocean warming: combined impact on physiology and surface properties of the marine microalga Dunaliella tertiolecta***" by Petra Vukosav, Bruno Komazec, Petra Peharec Štefanić, Darija Domazet Jurašin and Tea Mišić Radić for consideration for publication in the Marine Pollution Bulletin.

As the oceans continue to warm due to climate change, combined impacts of acean warming and emerging pollutants such as nanoplastics are becoming an increasing problem for marine ecosystems including microalgae as marine primary producers. Although the individual effects of nanoplastics and elevated temperature have been investigated, their combined effect is not yet well characterised. Only one very recent study has investigated the interaction of nanoplastics and heat stress on marine diatom *Chaetoceros gracilis* (Hou et al., 2025, https://doi.org/10.1016/j.jhazmat.2024.136703)

In our study, we investigated how these two stressors, increased temperature and nanoplastics, interact to affect marine microalga *Dunaliella tertiolecta*. We performed a comprehensive assessment at both the population and individual cell level. Specifically, we investigated the effects of short-term (5-day) exposure to amine-modified polystyrene nanoplastics (PS-NH_2 NPs, diameter 51 nm) and elevated temperature (30 °C) on the physiology and surface properties of *D. tertiolecta*. Our results show that PS-NH_2 NPs significantly inhibited algal growth at both 18 °C and 30 °C, with more pronounced inhibition and lower EC_{50} values at the higher temperature. At both temperatures, the nanoplastics triggered excessive production of reactive oxygen species (ROS), increased lipid peroxidation and stimulated the activity of important antioxidant enzymes. At the same time, photosynthetic performance decreased sharply, which was reflected in a reduction in the maximum quantum yield of PSII (F_v/F_m) and the performance index (PI_{abs}). In addition to the physiological effects, we investigated nanostructural and nanomechanical changes at the cellular level. While the PS-NH_2 NPs adhered to the algal cell surface at both temperatures, the changes in cell stiffness and adhesion were significant only at the

elevated temperature. At 30 °C, we observed a remarkable reduction in both mechanical parameters, suggesting that heat stress enhances the disruptive effect of nanoplastics on cell surface integrity, which may affect cell-environment interactions cell resistance and.

Overall, this study demonstrates the synergistic effects of nanoplastics and ocean warming on microalgae and provides new insights into the ecological risks that these combined stressors pose to marine primary producers in the context of future climate change. Furthermore, our results emphasize the importance of including multiple environmental variables, including temperature and co-occurring stressors, to improve the ecological risk assessment of nanoplastics under changing ocean conditions.

This manuscript represents original, unpublished work not considered elsewhere. All authors have approved the manuscript and consent to its publication. We declare no conflicts of interest.

We thank you for considering our manuscript for publication in Marine Pollution Bulletin. We believe it will be of interest to your readership and make an important contribution to the field of marine ecotoxicology and climate impact research. We would be happy to provide you with additional information or address the reviewers' comments if required.

Sincerely,

Tea Mišić Radić

Graphical Abstract

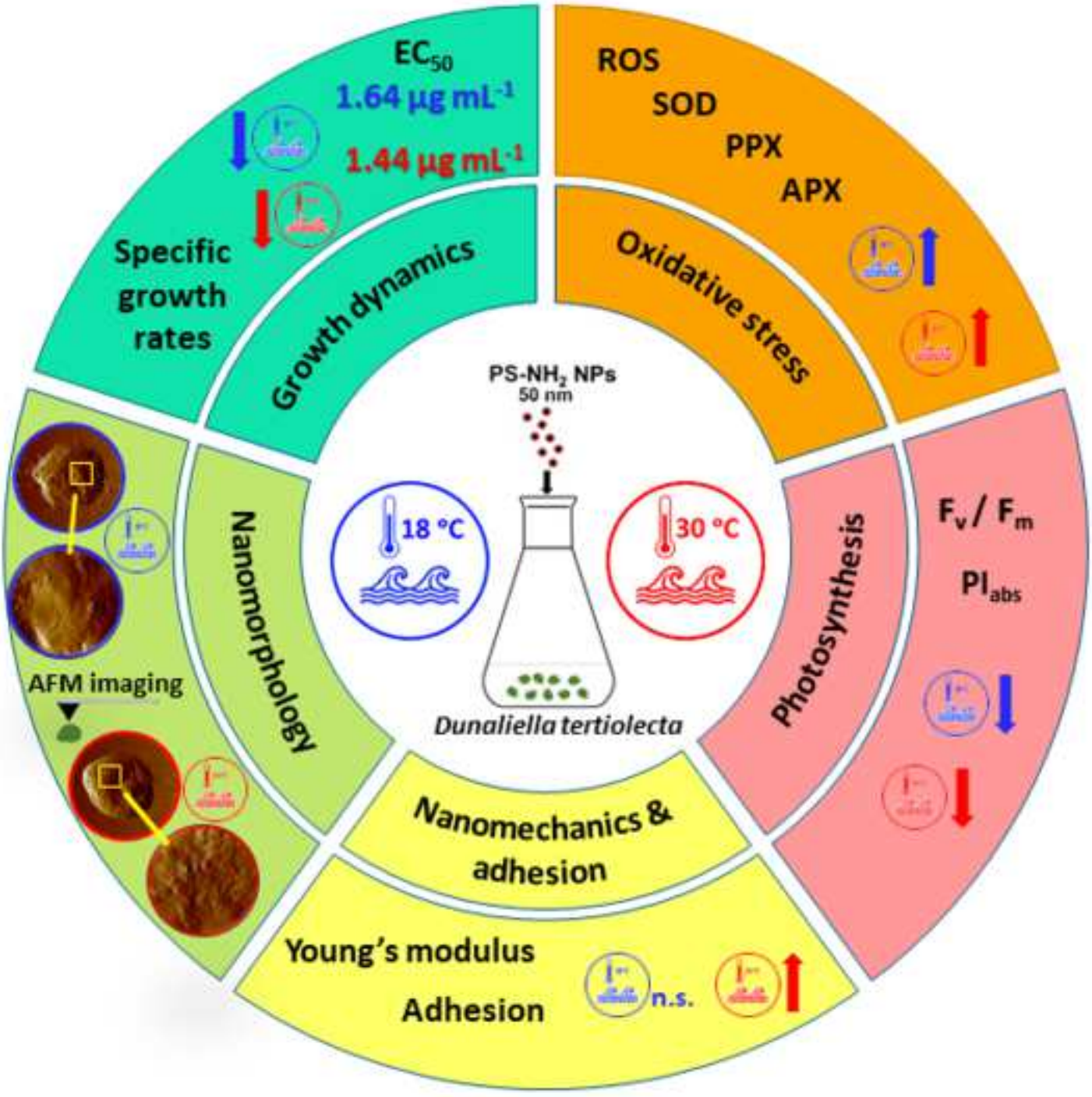

Highlights

- Ocean warming enhances growth inhibition of nanoplastics on *D. tertiolecta*
- Elevated temperature lowers EC_{50} of amine-modified polystyrene nanoplastics
- Increased ROS production and oxidative stress biomarkers at both temperatures
- Photosynthetic efficiency decreases under nanoplastic exposure at both temperatures
- Nanoplastics and warming significantly decrease cell stiffness and adhesion

Nanoplastics and ocean warming: combined impact on physiology and surface properties of the marine microalga *Dunaliella tertiolecta*

Petra Vukosav[a], Bruno Komazec[b], Petra Peharec Štefanić[b], Darija Domazet Jurašin[c], Tea Mišić Radić[a,*]

[a] Division for Marine and Environmental Research, Ruđer Bošković Institute, Bijenička 54, 10000 Zagreb, Croatia

[b] Department of Biology, Faculty of Science, University of Zagreb, Horvatovac 102a, 10000 Zagreb, Croatia

[c] Division of Physical Chemistry, Ruđer Bošković Institute, Bijenička 54, 10000 Zagreb, Croatia

* Correspondence: tmisic@irb.hr

Petra Vukosav - https://orcid.org/0000-0002-5946-055X ; e-mail: petra.vukosav@irb.hr

Bruno Komazec - https://orcid.org/0000-0002-9410-231X ; e-mail: bruno.komazec@biol.pmf.unizg.hr

Petra Peharec Štefanić - https://orcid.org/0000-0003-4889-6910 ; e-mail: petra.peharec.stefanic@biol.pmf.unizg.hr

Darija Domazet Jurašin - https://orcid.org/0000-0001-5261-5961 ; e-mail: darija.domazet.jurasin@irb.hr

Tea Mišić Radić - https://orcid.org/0000-0002-2523-4749 ; e-mail: tmisic@irb.hr

Abstract

Ocean warming due to climate change, in combination with emerging pollutants such as nanoplastics, poses a growing threat to marine ecosystems. This study investigates the combined impact of amine-modified polystyrene nanoplastics (PS-NH_2 NPs, diameter 51 nm) and elevated temperature (30 °C) on the physiology and surface properties of the marine green microalga *Dunaliella tertiolecta*. We assessed responses at both single-cell and population levels by examining growth dynamics, reactive oxygen species (ROS) production, oxidative stress biomarkers, photosynthetic efficiency and changes in nanostructural and nanomechanical cell properties. Short-term exposure (5 days) to PS-NH_2 NPs significantly inhibited algal growth at both 18 °C and 30 °C, with stronger inhibition and lower EC_{50} values at 30 °C. Nanoplastics induced excessive ROS production at both temperatures, leading to increased lipid peroxidation and increased activities of antioxidant enzymes. Photosynthetic performance decreased significantly at both temperatures as reflected by a lower maximum quantum yield of PSII (F_v/F_m) and a lower performance index (PI_{abs}). While the nanoplastics adhered to the surface of the algal cells at both temperatures, the effects on nanomechanical properties were temperature dependent. At 18 °C, the PS-NH_2 NPs had a negligible effect on cell stiffness and adhesion. However, simultaneous exposure to nanoplastics and elevated temperature significantly reduced both cell stiffness and adhesion, suggesting that heat stress enhances the adverse effect of nanoplastics on cell surface integrity. Overall, this study highlights how nanoplastics and ocean warming synergistically impact microalgae and provides new insights into the ecological risks posed to marine microalgae under future climate scenarios.

Keywords: microalga *Dunaliella tertiolecta*; nanoplastics; ocean warming; oxidative stress biomarkers; photosynthetic performance; cell nanomechanical properties

1. Introduction

The extensive use and improper disposal of plastic products have led to major ecological concerns, particularly due to the accumulation of plastics in the marine environment (European Comission, 2018). An estimated 5 to 13 million tons of plastic, representing around 1.5 to 4% of global plastic production, end up in the oceans every year (Jambeck et al., 2015). Moreover, it is estimated that plastics constitute more than 80% of marine litter (European Comission, 2018). At the same time, climate change is causing ocean warming, with worst-case scenarios predicting an increase in mean sea surface temperatures of up to 3 °C by the end of this century (Fox-Kemper et al., 2021). This is expected to be accompanied by an increase in the frequency, intensity and duration of extreme weather and climate events in the oceans, such as marine heatwaves (Capotondi et al., 2024). Both rising ocean temperatures and the intensification of marine heatwaves pose a serious threat to marine ecosystems and marine organisms, including microalgae.

Microalgae, as important primary producers in the ocean, form the basis of the marine food web and play an important role in maintaining the ecological balance of marine ecosystems. Therefore, understanding the effects of nanoplastics on marine microalgae is crucial to anticipate their impact on coastal marine food webs and the ecosystems they sustain. Due to their wide distribution, short life cycle and rapid response to environmental and anthropogenic stressors, microalgae can serve as effective indicators of environmental quality (Rimet, 2012; Tudesque et al., 2012). In recent years, a growing number of researchers have investigated the potential ecotoxicological impacts of nanoplastics on aquatic ecosystems, including impacts on microalgae (Gonçalves and Bebianno, 2021; Mišić Radić et al., 2022; Piccardo et al., 2020; Wang et al., 2020; Zaki et al., 2022). These studies mainly focused on growth inhibition, while fewer studies investigated oxidative stress and effects on photosynthesis (Bellingeri et al., 2019; Bergami et al., 2017; Bhattacharya et al., 2010; Chae et al., 2018; Gomes et al., 2020; Hazeem et al., 2020; Nolte et al. 2017; Sendra et al., 2019; Zhao et al., 2020). In our previous study, we showed that exposure of the marine diatom *Cylindrotheca closterium* to carboxyl- and amine-modified polystyrene nanoparticles resulted in growth inhibition and phytotoxic effects due to excessive ROS production, leading to increased oxidative damage to lipids and changes in antioxidant enzyme activities and changes in nanomechanical properties of the cells (Mišić Radić et al., 2022).

As the oceans continue to warm due to climate change, the combination of increased temperature and pollutants such as nanoplastics poses an increasing challenge to the functioning of the marine ecosystem. Although there are a growing number of studies on the effects of nanoplastics on microalgae, to our knowledge, only one recent study has investigated the combined effects of nanoplastics and ocean warming, i.e. heatwaves, on microalgae (Hou et al., 2025). Hou and coworkers showed that a temperature increase of 4 °C increases the toxicity of polystyrene NPs on the diatom *Chaetoceros gracilis*. Other previous research has mainly focused on the isolated effects of nanoplastics or temperature stress on marine microalgae.

This study aims to fill this gap by investigating the combined impacts of polystyrene nanoplastics and elevated temperature on the marine microalga *Dunaliella tertiolecta* (Butcher) (Chlorophyceae). Specifically, we will investigate how the combination of these two stressors affects growth dynamics, photosynthesis, oxidative stress responses and the nanostructural and nanomechanical properties of *D. tertiolecta*. By studying the interaction between plastic pollution and climate change-induced ocean warming, this research will improve our understanding of how nanoplastics affect marine microalgae under global

warming conditions, which is essential for predicting future broader ecological consequences of nanoplastic pollution in the marine environment.

2. Materials and methods

2.1. Polystyrene nanoparticles characterization

Amine-modified polystyrene nanoparticles (PS-NH_2 NPs) were purchased from Polysciences (Warrington, PA, USA). The stock suspension was supplied as a 10% (w/w) solid suspension in deionized water with a small amount of surfactant (<0.05% SDS). The nominal diameter of PS-NH_2 NPs specified by the manufacturer was 51 nm. Before use, the stock suspension was vortexed for 1 minute and diluted with ultrapure water (UPW) to a concentration of 1% (w/w) and again briefly vortexed. This diluted stock was then used to prepare final PS-NH_2 NPs suspensions either in UPW or in filtered natural seawater (FSW; salinity 39, pH 8.0) at a final concentration of 50 μg mL^{-1} by brief vortexing (1 minute). To assess the thermal stability, the suspensions were incubated at 18 °C and 30 °C and characterized after 24 hours and 5 days.

The particle size distribution, i.e. hydrodynamic diameter (d_h) and zeta potential (ζ) of PS-NH_2 NP suspensions in UPW and FSW were determined by dynamic light scattering (DLS) and electrophoretic light scattering (ELS). DLS and ELS measurements were performed using a photon correlator spectrophotometer equipped with a 532 nm green laser (Zetasizer Nano ZS, Malvern Instruments Ltd., Worcestershire, UK). The d_h was determined as the value at the peak maximum of the volume size distribution. All reported results represent the average of six measurements. Data processing was performed using Zetasizer software version 7.13 (Malvern Instruments).

Visualization of PS-NH_2 nanoparticles in UPW and FSW was performed using a FEI Morgagni 268D transmission electron microscope (FEI, Hillsboro, Oregon, USA). Formvar®/carbon copper grids were used for imaging. One drop of a suspension of PS-NH_2 nanoparticles was placed on each grid and the samples were incubated for 5 minutes to allow precipitation of the particles. After incubation, the excess solution was removed with filter paper, the grids were carefully air-dried and then visualized with TEM to analyse the morphology of the nanoparticles.

2.2. Microalgal culture

The microalga *Dunaliella tertiolecta* (Chlorophyceae) (Butcher) was obtained from Culture Collection of the Bigelow Laboratory for Ocean Sciences (East Boothbay, ME, USA). *D. tertiolecta* was grown in Erlenmeyer flasks (250 mL) in 100 mL of f/2 medium (Guillard et al., 1975). Seawater from the Adriatic Sea (2 km offshore the island of Vis, 25 m depth), previously filtered through cellulose nitrate membrane filter (0.2 μm pore size; Whatman; Cytiva, Marlborough, MA) was used for the preparation of f/2 medium. A water bath with constant shaking (20 rpm) and a 12:12 light:dark (L:D) cycle at an irradiance of 31 μmol photons m^{-2} s^{-1} was used for growing of microalgae cultures. The temperature of the water bath was kept constant at 18 °C or 30 °C.

2.3. Exposure experiment

D. tertiolecta monocultures were exposed to selected concentrations of amine-modified polystyrene nanoplastics (PS-NH_2 NPs) for 5 days under controlled laboratory conditions at two temperatures: 18 °C and 30 °C. Erlenmeyer flasks with f/2 medium were

inoculated with the algal culture in the exponential growth phase (five days old) and spiked with PS-NH_2 NPs. The concentration range of NPs (1.0, 1.5, 2.0 and 3.0 μg mL^{-1}) was determined based on preliminary EC_{50} value (concentrations that resulted in a 50% reduction in growth) determined at both temperatures, with the highest concentration being slightly higher than the corresponding EC_{50} values. A control culture, which was not spiked with nanoplastics, was maintained under identical conditions. All treatments, including the controls, were started at a cell density of approximately 5×10^4 cells mL^{-1} and performed in triplicate.

2.4. Growth dynamics

Algal cell density was counted microscopically using a Luna II™ Automated Cell Counter (Logos Biosystems Inc, now Aligned Genetics Inc, Anyang-si, South Korea). The following equations were used to determine the percentage of growth inhibition (%*I*) and the average specific growth rate ($\mu_{i\text{-}j}$) for a given time period (OECD, 2011):

$$\mu_{i\text{-}j} = \frac{\ln N_j - \ln N_i}{t_j - t_i} d^{-1} \quad (1)$$

$$\%\, I = \frac{\mu_C - \mu_T}{\mu_C} \times 100 \quad (2)$$

where $\mu_{i\text{-}j}$ is the average specific growth rate (expressed in units of d^{-1}) from time i to j; t_i and t_j correspond to the time of the beginning and end of the period, respectively; N_i and N_j are the number of cells per culture volume at time i and j, respectively; % *I* is the growth inhibition expressed as a percentage; μ_C is the average specific growth rate of the control group and μ_T is the specific growth rate for the treatment replicate. The effective concentrations of PS-NH_2 NPs resulting in a 50% reduction in growth (EC_{50}) at temperatures of 18 °C and 30 °C were calculated by plotting *I* against the logarithm of the concentration of the nanoplastics and fitting to the logistic equation (OECD, 2011).

2.5. Determination of reactive oxygen species (ROS)

The ROS content in all samples was determined using two fluorescent probes: dihydroethidium (DHE) and 2',7'-dichlorofluorescein diacetate (H_2DCFDA) according to previously published protocols (Cvjetko et al., 2017; Hong et al., 2009). In brief, a stock solution of each probe was prepared at a concentration of 10 μM, of which 20 μL was mixed with 180 μL of algal suspension. After incubating the samples in complete darkness for 30 min, the fluorescence signal was detected using a GloMax microplate reader (Promega, Madison, WI, USA). Excitation/emission wavelengths of 520/600 nm were used for DHE, while values of 504/550 nm were used for H_2DCFDA. Fluorescence intensity was adjusted according to the cell concentration in each sample, and the results are expressed as percentages relative to control samples.

2.6. Determination of antioxidant enzyme activities and malondialdehyde (MDA) content

2.6.1. Protein extraction

To extract total soluble proteins, *D. tertiolecta* cells were first centrifuged at 2000 × g at 20 °C for 3 minutes. The resulting pellet was washed three times with FSW, with the cells being centrifuged again under the same conditions after each wash. After the last wash, the

cells were homogenized three times in 500 µL of 50 mM potassium phosphate buffer (pH 7.0) with the addition of glass beads (size 425–600 µm), using a Retsch homogenizer (model MM200, Retsch, Haan, Germany) at 30 Hz for 3 minutes at 4 °C. The resulting cell homogenates were then first centrifuged at 20,817 × g for 15 minutes at 4 °C, and the supernatants were further purified by a second centrifugation under the same conditions for 45 minutes. The protein concentration in the resulting extracts was determined by the Bradford method (Bradford, 1976), using bovine serum albumin to generate a standard curve, and the samples were then used for analysis of specific enzyme activity.

2.6.2. Enzymatic activity assays

The specific antioxidant enzyme activity analyses were performed using a UV/VIS spectrophotometer (ATI UNICAM UV4, Cambridge, UK) at room temperature (25 °C) and the enzyme activity values were normalized to the concentration of total soluble proteins in the sample.

The activity of pyrogallol peroxidase (PPX, EC 1.11.1.7) was determined by the oxidation of pyrogallol in the presence of the PPX enzyme, resulting in an increase in absorbance at a wavelength of 430 nm (ε = 2.6 mM^{-1} cm^{-1}) (Nakano and Asada, 1981). 20 µL of the protein extract was added to 980 µL of a reaction mixture consisting of 50 mM potassium phosphate buffer (pH 7.0), 20 mM pyrogallol and 5 mM H_2O_2, and the change in absorbance was measured for two minutes.

For the determination of ascorbate peroxidase (APX, EC 1.11.1.11) activity, a previously described protocol was used (Nakano and Asada, 1981), with the decrease in absorbance at 290 nm (ε = 2.8 mM^{-1} cm^{-1}) serving as an indicator of PPX enzyme activity. Briefly, 180 µL of the protein extract was added to 820 µL of a reaction mixture containing 50 mM potassium phosphate buffer (pH 7.0), 0.5 mM ascorbate, and 10 mM H_2O_2, and the absorbance was measured for one minute.

Catalase activity (CAT, EC 1.11.1.6) was measured based on the decrease in H_2O_2 absorbance in the presence of the CAT enzyme in the reaction mixture at 240 nm (ε = 36 mM^{-1} cm^{-1}) (Aebi, 1984). In brief, 950 µL of the reaction mixture (50 mM potassium phosphate buffer (pH 7.0) and 20 mM H_2O_2) was mixed with 50 µL of protein extract and the change in absorbance was measured for one minute.

2.6.3. Malondialdehyde content

To determine the intensity of lipid peroxidation in *D. tertiolecta* after treatment, the content of its indirect indicator malondialdehyde (MDA) was measured spectrophotometrically (Heath and Packer, 1968). Briefly, 100 mL of the algal cell suspension was first centrifuged at 2000 × g for 3 min at 20 °C. The cell pellet was washed three times with FSW, with the cells being centrifuged again under the same conditions after each wash. After the last wash, the cells were homogenized three times in 700 µL of a 0.5% (w/v) 2-thiobarbituric acid solution prepared in 20% (w/v) trichloroacetic acid with the addition of glass beads (size 425–600 µm) using a Retsch homogenizer (model MM200, Retsch, Haan, Germany) at 30 Hz for 3 min at 20 °C. The resulting homogenate was then incubated at 95 °C for 30 minutes. The samples were then cooled and centrifuged at 14,000 × g at 4 °C for 30 minutes. The absorbance of the resulting supernatants was measured at 532 and 600 nm to eliminate the effects of non-specific turbidity by subtracting the absorbance at 600 nm from

the absorbance at 532. The results were then normalized to the same cell concentration in all samples.

2.7. Photosynthesis parameters

To determine the photosynthetic parameters, specifically the chlorophyll *a* fluorescence parameters, including the maximum quantum yield of photosystem II (PSII) (F_v/F_m) and its performance index (PI_{abs}), the concentration of cells in the samples was first measured. An equal number of cells in each sample were incubated in complete darkness for 30 minutes to allow complete oxidation of PSII and to exclude non-photochemical quenching. After incubation in the dark, 3 mL of the suspension was added to special cuvettes of the AquaPen instrument (Photon Systems Instruments, Drásov, Czech Republic) and the fluorescence of chlorophyll *a* was measured with the OJIP test using a superpulse with an intensity of 53%. The data obtained were processed in FluorPen software version 1.1.1.3 (Photon Systems Instruments, Drásov, Czech Republic) and expressed as the ratio of variable to maximum fluorescence (F_v/F_m) and as PSII efficiency index (PI_{abs}) in arbitrary units.

2.8. Atomic force microscopy working in force spectroscopy mode

AFM measurements of the physical properties of the cells (cell elasticity and adhesion) were performed using the JPK NanoWizard 4 XP AFM system (Bruker, Billerica, MA, USA) coupled to the inverted fluorescence microscope Olympus IX 73 (Olympus, Tokyo, Japan). The force spectroscopy experiments were performed with Bio-MLCT cantilevers (Bruker, Billerica, MA, USA; nominal spring constant of 0.03 N m^{-1}). The sensitivity and spring constants of cantilevers were determined before each experiment using the thermal noise method (Sader et al., 1995). The force curves were recorded in the central region of the cell body within a scan area of 1 µm × 1 µm, within which a grid of 10 × 10 points was defined. The force curves were recorded at an approach and retract velocity of 2 µm s^{-1}, a maximum force of 0.5 nN and a curve length of 2 µm. The measurements were performed in seawater at room temperature. In each condition, 100 force curves were recorded on 10 different cells, in total, approximately 1000 curves were acquired per condition. The recorded force curves were analysed using JPK Data Processing Software (version 8.0.159, Bruker, Billerica, MA, USA) to determine the values of Young's moduli and work of adhesion.

Young's moduli were determined from 200 nm indentation curves using the Hertz model (Hertz, 1882), in which the force F, indentation (δ) and Young's modulus (Y_m) follow equation (3):

$$F = \frac{2 \times Ym \times \tan\alpha}{\pi \times (1-\upsilon^2) \times \delta^2} \quad (3)$$

where α is the opening angle of the tip (35°) and υ is the Poisson's ratio (arbitrarily assumed to be 0.5). To quantify the adhesion properties of the algal cells, the retract part of the force curve was analysed. As a result, a maximum work of adhesion (W_{adh}) was determined, which was defined as the area encompassing the negative force values.

For the measurements, cells from control or exposed culture grown at 18 °C and 30 °C were immobilized on Petri dishes coated with polyethylenimine (PEI). To modify the Petri dishes with PEI, 100 µL of 0.2% PEI was incubated on a clean Petri dish and left overnight. The next day, 100 µL of cell suspension was deposited on the dried PEI surface and allowed to

stand for at least 30 minutes before rinsing with FSW. After rinsing, the Petri dish was filled to half with FSW to perform the measurements.

AFM force curves obtained for individual cells are available in the FULIR DATA open repository (https://data.fulir.irb.hr/islandora/object/irb%3A732; urn:nbn:hr:241:147494).

2.9. Atomic force microscopy imaging

For AFM imaging of *D. tertiolecta* cells, Multimode Scanning Probe Microscope with Nanoscope IIIa controller (Bruker, Billerica, MA, USA) was used with a vertical engagement (JV) 125 µm scanner. Topographic images of the cell surface of *D. tertiolecta* were acquired in contact mode using silicon-nitride tips (DNP-10, Bruker, nominal frequency 12-24 kHz, spring constant of 0.06 N m^{-1}). The linear scanning rate was optimized between 1.0 and 2.0 Hz for imaging in contact mode with a scan resolution of 512 samples per line. NanoScope™ software (Bruker, NanoScope Analysis ver. 3.0) was used for image processing and analysis. All images are presented as raw data, except for the first-order two-dimensional flattening. All measurements were performed in air at room temperature and 30–40% relative humidity.

To prepare samples of *D. tertiolecta* for AFM imaging of cells, 1 mL of the cells were taken from 5 days old cultures (exponential phase) growing at 18 °C and at 30 °C that were not spiked with PS-NH_2 NPS (control cultures) and from the cultures spiked with PS-NH_2 NPs (2 µg mL^{-1}). A volume of 5 µL of the cell culture (previously fixed with formaldehyde) was pipetted directly onto freshly cleaved mica. To give the cells time to settle and adhere to the surface, the mica sheets were kept in closed Petri dishes for 45 minutes. The samples were then rinsed three times in ultrapure water and placed again in Petri dishes to evaporate the excess water. The diatom cells adhered securely to the mica surface using the sample preparation method described and allowed stable conditions for AFM experiments.

2.10. Data analysis

For the statistical analysis of the results for nanomechanical properties (Young's modulus and work of adhesion) Kruskal–Wallis test was used, followed by the Dunn's post-hoc test was performed. All analyses were performed in R (version 4.4.0, R Core Team, 2024) with RStudio (version 2024.04.1; Posit PBC, Boston, MA, USA) using the FSA package. For the analysis of ROS content, enzymatic antioxidant activity, lipid peroxidation level and photosynthetic parameters, a statistical analysis was performed using a one-way ANOVA test, followed by the Newman-Keuls post hoc test using the STATISTICA 14.0.0.15 software package (TIBCO Software, Inc., Palo Alto, CA, USA). Differences between the mean values were considered statistically significant at $p \leq 0.05$.

3. Results

3.1. Characterization of nanoplastics

Physicochemical and morphological characterization of PS-NH_2 NPs suspended in ultrapure water and natural filtered seawater at 18 °C and 30 °C was performed using DLS, ELS and TEM. The DLS/ELS data for the hydrodynamic diameter (d_h) and zeta potential (ζ) of the PS-NH_2 NPs suspensions showed that the particles exhibited colloidal stability for up to five days under all tested conditions (Table 1).

In UPW, the measured d_h was confirmed to be the average size reported by the supplier, averaging 47.4 ± 2.3 nm at 18 °C and 50.6 ± 0.9 nm at 30 °C. In FSW, the particles were slightly

larger, with d_h values of 54.4 ± 1.1 nm at 18 °C and 58.2 ± 0.9 nm at 30 °C. In addition to the main particle population, a very small percentage of larger aggregates (~ 5 µm, < 5 vol. %) were also detected in FSW at both temperatures. In terms of particle charge, the ζ-potential remained positive in both media and at both time points, but was significantly lower in FSW compared to UPW (Table 1). The TEM images also confirmed the presence of predominantly individually dispersed PS-NH_2 nanoparticles in both UPW and FSW suspensions at 18 °C and 30 °C (Fig. 1). In UPW, the TEM images showed nanoparticles with diameters between 47.5 nm and 55.3 nm. In FSW, the particles at both temperatures also remained mostly as single particles, with diameters ranging from 60.5 nm to 69.5 nm

3.2. Effect of nanoplastics on growth

The growth curves of *D. tertiolecta* exposed to PS-NH_2 nanoplastics (0–3 µg mL^{-1}) at 18 °C (a) and 30 °C (b) over a period of 5 days are shown in Fig. 2. Control cultures showed typical positive exponential growth from day 1 to day 5 at both temperatures. Cultures exposed to 1 µg mL^{-1} and 1.5 µg mL^{-1} PS-NH_2 NPs also showed positive growth at both temperatures, with exponential growth beginning on day 1 for cultures grown at 18 °C and on day 2 for cultures grown at 30 °C. Culture exposed to 2.0 µg mL^{-1} PS-NH_2 NPs and grown at 18 °C maintained positive growth during the first 2 days, followed by a plateau until day 5. In contrast, culture grown at 30 °C and exposed to 2.0 µg mL^{-1} PS-NH_2 NPs showed minimal changes in cell density over the entire 5-day period. Exposure to the highest PS-NH_2 NPs concentration (3.0 µg mL^{-1}) resulted in negative growth at both temperatures.

The specific growth rates (μ) and percentage of growth inhibition *(%I*) of *D. tertiolecta,* calculated using equations (1) and (2*),* for both the control and nanoplastics-treated cultures grown at 18 °C and 30 ° are shown in Table S1 (Supplementary Material). At 18 °C, the control culture showed consistently higher specific growth rates compared to the control culture grown at 30 °C over a period of five days. However, the growth rate of the cultures grown at 18 °C gradually decreased over time, from 0.45 d^{-1} on day 1 to 0.31 d^{-1} on day 5. In contrast, the control cultures grown at 30 °C showed an increasing growth rate over time, from 0.11 d^{-1} on day 1 to 0.29 d^{-1} on day 5. Increasing the PS-NH_2 NPs concentration from 0 to 3.0 µg mL^{-1} resulted in a decrease in the specific growth rate at both temperatures. At 18 °C, increasing the PS-NH_2 NPs concentration from 0 to 3.0 µg mL^{-1} resulted in a decrease in the specific growth rates, i.e. on day 5, the control culture had a growth rate of 0.31 d^{-1} (corresponding to a division rate of 0.45 div d^{-1}), while the culture exposed to the highest nanoplastics concentration (3.0 µg mL^{-1}) had a negative growth rate of −0.22 d^{-1} (−0.32 div d^{-1}). A similar pattern was observed in cultures grown at 30 °C. The specific growth rate on day 5 of the control culture was 0.29 d^{-1} (0.42 div d^{-1}), while the culture treated with 3.0 µg mL^{-1} PS-NH_2 NPs showed a negative growth rate of -0.27 d^{-1} (0.39 div d^{-1}).

At both temperatures, growth inhibition increased with increasing nanoplastic concentration during the 5-day experiment, with higher growth inhibition observed in cultures grown at 30 °C. For cultures grown at 30 °C, inhibition ranged from 85.0 % (for 1.0 µg mL^{-1} PS-NH_2 NPs) to 192.9% (for 3.0 µg mL^{-1} PS-NH_2 NPs), while for cultures grown at 18 °C, inhibition values ranged from 6.6 % (for 1.0 µg mL^{-1} PS-NH_2 NPs) to 171.4% (for 3.0 µg mL^{-1} PS-NH_2 NPs). The calculated effective concentrations of PS-NH_2 nanoplastics that resulted in a 50% reduction in growth over a 5-day period (EC_{50}) were calculated to be 1.64 µg mL^{-1} for *D. tertiolecta* cultures grown at 18 °C and 1.44 µg mL^{-1} for cultures grown at 30 °C.

3.3. *In situ* ROS formation

The ROS content determined with the fluorescent probes H_2DCFDA and DHE showed a concentration-dependent increase after exposure to nanoplastics at both tested temperatures (Fig. 3). The PS-NH_2 NPs concentration of 1.0 µg mL^{-1} did not cause significant changes in ROS production for both probes and at both temperatures compared to the control. At 18 °C, a statistically significant increase in ROS levels was observed at PS-NH_2 NPs concentrations of 1.5 and 2.0 µg mL^{-1}, for both probes. At 30 °C, the results obtained with H_2DCFDA showed a significant increase in ROS at 1.5 µg mL^{-1} and 2.0 µg mL^{-1}, while the analysis with the DHE probe showed a significant increase only at the highest PS-NH_2 NPs concentration (2.0 µg mL^{-1}).

3.4. Antioxidant enzyme activity

The specific activities of the antioxidant enzymes PPX, APX and CAT varied significantly depending on the temperature and the concentration of PS-NH_2 nanoplastics (Fig. 4). PPX activity (Fig. 4A) showed a statistically significant increase at all nanoparticle concentrations at 18 °C compared to the control. At 30 °C, PPX activity increased only at higher concentrations (1.5 and 2.0 µg mL^{-1}), but this increase was less pronounced than at the lower temperature. APX activity (Fig. 4B) also showed a sensitive response to treatment. At 18 °C, all treatments resulted in increased activity compared to the control, with the concentrations of 1.5 and 2.0 µg mL^{-1} inducing the strongest response. At 30 °C, only these two higher concentrations caused a significant increase compared to the control, but the values were significantly lower than those measured at 18 °C for the corresponding treatments. CAT activity (Fig. 4C) showed a significant increase at 18 °C for all concentrations of nanoplastics compared to control. At 30 °C, an increase in activity was also observed for all treatments, with the 1.0 µg mL^{-1} treatment causing the smallest increase and the 1.5 µg mL^{-1} treatment causing the largest increase. Nevertheless, CAT activity was significantly higher at 18 °C than at 30 °C, even in the control group.

3.5. Effect on lipid perodixation

Lipid peroxidation, expressed as MDA levels, changed significantly depending on temperature and nanoparticle concentration (Fig. 5). At 18 °C, a concentration-dependent increase in lipid peroxidation was observed. All treatments resulted in significantly higher MDA levels compared to the control, with the highest concentration (2.0 µg mL^{-1}) causing the greatest increase. At 30 °C, all treatments also led to a significant increase in lipid peroxidation compared to the control, but the differences between the individual concentrations were less pronounced. Although a slight decrease in MDA was observed at the highest treatment concentration (2.0 µg mL^{-1}) compared to the same treatment at 18 °C, lipid peroxidation levels remained elevated in all treated samples.

3.6. Effect of nanoplastics on photosynthesis

Measurements of the maximum quantum yield of photosystem II (F_v/F_m) and the fluorescence performance index (PI_{abs}) showed concentration and temperature dependent changes in the photosynthetic efficiency of the cells (Fig. 6). At both temperatures, treatments with 1.0 µg mL^{-1} caused no significant decrease in F_v/F_m compared to the control, while treatments with 1.5 µg mL^{-1} and 2.0 µg mL^{-1} resulted in statistically significant decreases, with the largest decrease observed at the highest concentration (2.0 µg mL^{-1}). A similar pattern was observed for PI_{abs}. At 18 °C, treatment with nanoplastic concentration of 1.0 µg

mL^{-1} did not significantly alter PI_{abs} values, whereas treatments with 1.5 µg mL^{-1} and 2.0 µg mL^{-1} caused a significant decrease, with the decrease again being most pronounced at the highest concentration. However, at 30 °C, only treatment with nanoplastic concentration of 2.0 µg mL^{-1} resulted in a statistically significant decrease in PI_{abs} compared to the control, but this decrease was less pronounced than at the same concentration at 18 °C.

3.7. Interaction of nanoplastics with algal cells

Atomic force microscopy (AFM) was used to investigate the interaction between nanoplastics and *D. tertiolecta* at the single cell level. Cells were sampled from control cultures and from cultures exposed to PS-NH_2 NPs at concentrations slightly above the corresponding EC_{50} value (2.0 µg mL^{-1}) during the exponential growth phase (day 5). AFM imaging showed that the *D. tertiolecta* cells of both control and nanoplastics-treated cultures had a typical ovoid morphology with two flexible flagella at both temperatures (Fig. 7), which is consistent with previous observations (Novosel et al., 2022a; 2022b). Cell dimensions remained the same in all treatments, with lengths ranging from 10.07 to 10.85 µm, central widths from 7.36 to 8.29 µm and central heights from 1.59 to 1.99 µm (Supplementary Material, Table S2).

At 18 °C, the PS-NH_2 NPs were observed as single particles adsorbed on the cell surface (Fig. 7C, D). In contrast, AFM images at 30 °C showed that PS-NH_2 NPs formed aggregates on the surface of the exposed cells (Fig. 7G, H), indicating temperature-dependent differences in particle–cell interactions. Despite the presence of nanoparticles, no significant changes in surface nanostructure or morphology were observed in the treated cells compared to controls at either temperature (Fig. 7A, B, E, F).

3.8. Effect of nanoplastics on the nanomechanical properties

To quantitatively assess the nanomechanical properties of *D. tertiolecta*, the Young's modulus (Y_m) and work of adhesion (W_{adh}) were determined using atomic force microscopy in force spectroscopy mode. In this mode, the AFM generates force–distance curves by plotting the force exerted by the cantilever tip against its displacement relative to the sample surface (Fig. 8A, B). These curves can be analysed using mathematical models to extract important mechanical properties of the cell surface. In particular, Y_m is derived from the slope of the approach curve in the contact region, while the adhesion force corresponds to the maximum negative force observed during the retraction phase. The work of adhesion, W_{adh}, is calculated as the area between the retraction curve and the baseline.

Cells from control cultures and those exposed to PS-NH_2 NPs (2.0 µg mL^{-1}) were harvested on day 5 of cultivation at 18 °C and 30 °C. The results of AFM force spectroscopy measurements are shown in Fig. 8C, D. At 30 °C, the mean Y_m value of the control cells (8.687 ± 5.903 kPa) was slightly lower than at 18 °C (9.000 ± 6.109 kPa), indicating a minor reduction in cell stiffness, however, this difference was not statistically significant. Similarly, at 18 °C, no significant difference in stiffness was observed between the control cells (9.000 ± 6.109 kPa) and the cells exposed to nanoplastics (9.124 ± 6.238 kPa). However, at 30 °C, exposure to PS-NH_2 NPs resulted in a significant decrease in cell stiffness, with Y_m decreasing from 8.687 ± 5.903 kPa in the control cells to 7.998 ± 5.684 kPa in the exposed cells.

A similar pattern was observed for adhesion. At 18 °C, there was no significant difference in W_{adh} between the control cells (0.01633 ± 0.022 fJ) and the nanoplastics-exposed cells (0.014 ± 0.029 fJ). In contrast, nanoplastic exposure at 30 °C significantly

decreased adhesion; W_{adh} decreased from 0.04779 ± 0.0448 fJ in control cells to 0.015 ± 0.0149 fJ in treated cells. In addition, temperature alone had a significant effect on adhesion, with control cells grown at 30 °C exhibiting significantly higher W_{adh} than cells grown at 18 °C.

4. Discussion

As the oceans continue to warm due to climate change, emerging pollutants such as nanoplastics are becoming an increasing problem for marine ecosystems including microalgae as marine primary producers. In this study, we investigated the combined impact of nanoplastics and global warming related temperature increase on the marine green microalga *Dunaliella tertiolecta*. Under controlled laboratory conditions, *D. tertiolecta* cultures were grown at two temperatures (18 °C and 30° C) and exposed to different concentrations of amine-modified polystyrene nanoparticles (PS-NH_2 NPs, diameter 51 nm) to evaluate physiological, nanostructural and nanomechanical responses. The size of the nanoparticles and their colloidal stability at 18 °C and 30 °C were characterized by DLS/ELS and TEM. The results confirmed the colloidal stability of PS-NH_2 nanoparticles in both ultrapure water and seawater, with the particles mostly appearing as single particles. A small fraction of microaggregates observed in FSW at both temperatures is probably due to a reduced zeta potential resulting from the higher ionic strength of seawater promoting particle aggregation.

In terms of growth dynamics, *D. tertiolecta* grew slightly slower at 30 °C compared to 18 °C in both the control and treated groups, which is consistent with previously reported thermal limitations in this species (Novosel et al., 2022b). Exposure to PS-NH_2 NPs resulted in concentration-dependent growth inhibition at both temperatures, although stronger inhibition was observed at 30 °C, indicating a synergistic interaction between the toxicity of nanoplastics and thermal stress. Similar growth inhibitory effects of PS-NH_2 NPs on *D. tertiolecta* have already been reported (Bergami et al., 2017). In addition, growth inhibition has been documented in other microalgae species exposed to amine-modified polystyrene nanoparticles (Casado et al. 2013; González-Fernández et al., 2020, Hanachi et al., 2022; Hou et al., 2025; Khoshnamvand et al., 2021, 2024; Mišić-Radić et al. 2022; Nolte et al. 2017). Interestingly, *D. tertiolecta* was also sensitive to unmodified polystyrene nanoparticles (Sjollema et al., 2016), while no adverse effects were reported for carboxyl-modified polystyrene nanoparticles despite their adsorption on the algal surface (Bergami et al., 2017), suggesting that surface chemistry plays a key role in the toxicity of nanoplastics.

In addition to the effects on growth dynamics, exposure to PS-NH_2 NPs at both temperatures resulted in a concentration-dependent increase in reactive oxygen species (ROS) production, lipid peroxidation levels and antioxidant enzyme activity. These results are consistent with previous reports (Jalaudin Basha et al., 2023; Zhu et al., 2021). At the same time, photosynthetic performance was impaired, as evidenced by a decrease in the maximum quantum yield of PSII (F_v/F_m) and power index (PI_{abs}). These observations are in line with previous studies showing that PS-NH_2 NPs induce oxidative stress and impair photosynthetic efficiency in various microalgal species. For example, *Alexandrium tamarense* exposed to PS-NH_2 NPs showed elevated ROS levels, increased activities of antioxidant enzymes and non-enzymatic antioxidants, and a decrease in photosynthetic efficiency (Li L. et al., 2024). Similarly, PS-NH_2 NPs in *Navicula* sp. triggered lipid peroxidation and altered the expression of genes related to thylakoid membranes and the photosynthetic apparatus (Li X. et al., 2024). Our results confirm these findings, although some studies have reported an increase in F_v/F_m levels in certain marine microalgae upon exposure to nanoplastics (Wang et al., 2020), suggesting possible species-specific dependent responses.

Although ROS levels were comparable between 18 °C and 30 °C in our study, lipid peroxidation and antioxidant enzyme activity were more pronounced at 18 °C. This suggests that elevated temperature can activate cellular protective mechanisms that mitigate oxidative damage. Microalgae possess various thermotolerant adaptations, such as increased carotenoid synthesis and expression of heat shock proteins, which contribute to stabilizing proteins, protecting membrane integrity and reducing oxidative stress (Abassi et al., 2020; Jolly, 2018; Kumari et al., 2022). Previous studies have shown that elevated temperatures increase metabolic activity in *Schizochytrium* sp. including antioxidant defenses and cellular repair mechanisms (Hu et al., 2021). Furthermore, using computational modeling, López Muñoz and Bernard (2021) have shown that higher temperatures reduce susceptibility to oxidative stress by promoting antioxidant synthesis, enzymatic activity and ROS scavenging, which ultimately contributes to greater stability of photosystem II. In our study, this was reflected in the smaller decrease in photosynthetic performance at 30 °C compared to 18 °C.

Adsorption of nanoplastic particles on the surface of microalgae is considered to be a key mechanism for disrupting photosynthesis, primarily by limiting light availability to thylakoid membranes (Bhattacharya et al., 2010; Wang et al., 2019). Using atomic force microscopy (AFM), we confirmed the adsorption of PS-NH_2 NPs on the surface of *D. tertiolecta*, which appeared as individual particles at 18 °C and as aggregates at 30 °C. This observation is consistent with our previous study in which AFM showed the adsorption of PS-NH_2 NPs on *Cylindrotheca closterium* (Mišić Radić et al., 2022). Other studies investigating the interaction between differently functionalized polystyrene NPs and green algae such as *Pseudokirchneriella subcapitata* and *Chlorella vulgaris* have shown that positively charged and neutral nanoplastic particles adhere more strongly to the algae cell walls than negatively charged ones (Hazeem et al., 2020; Nolte et al., 2017), highlighting the importance of surface chemistry in nanoparticle-algae interactions.

A comparison of the elasticity of *D. tertiolecta* control cells at 18 °C and 30 °C revealed a slight, although not significant, decrease, in the modulus of elasticity at the higher temperature, indicating a lower stiffness of the cells. This trend is consistent with the results of Novosel et al. (2022b), who reported a temperature-induced softening of *D. tertiolecta* cells. However, the absolute values of the elastic modulus in our study (9.0 kPa at 18 °C and 8.7 kPa at 30 °C) were significantly higher than those reported by Novosel et al. (3.5 kPa and 1.5 kPa, respectively). This discrepancy is probably due to differences in the physiological state of the cells, as our measurements were performed in the exponential growth phase, whereas Novosel et al. examined the cells in the stationary phase. Previous studies have also shown that *D. tertiolecta* loses elasticity with age, which is likely due to structural changes in the cell envelope (Pillet et al., 2019). The obtained results from the nanoplastics exposure experiments, showed that the exposed cells maintained similar elastic properties to the control cells at 18 °C, suggesting that PS-NH_2 NPs have no effect on cell mechanics at this temperature. However, at 30 °C, a decrease in stiffness was observed, which was more pronounced after exposure to PS-NH_2 NPs. Although the decrease in cell stiffness at 30 °C was not statistically significant in unexposed cells, the significant decrease upon combined thermal and nanoplastic exposure indicates a synergistic weakening of the cell surface. These results suggest that elevated temperature may increase the disruptive effect of nanoplastics on cell surface integrity and make cells more vulnerable. To date, data on the nanomechanical properties of *D. tertiolecta* exposed to nanoplastics are lacking, and similar studies on other microalgae remain limited (Mišić-Radić et al., 2022; Hou et al., 2025). Our previous work on *Cylindrotheca closterium* also showed a reduction in elastic modulus after exposure to

nanoplastics (Mišić-Radić et al., 2022), supporting the notion that nanoplastics impair cell wall integrity in various microalgal taxa. In addition, Hou et al. (2025) have recently shown that *Chaetoceros gracilis* exhibits decreased stiffness and increased adhesion under heat wave conditions, further confirming the synergistic effects of thermal and nanoparticle stress on the mechanical properties of algae. In our study we also showed that temperature had a significant effect on adhesion, with adhesion of cells from the control culture grown at 30 °C being significantly higher (0,04779 +- 0,0448 fJ) than adhesion of cells grown at 18 °C (0,01633+-0,022 fJ), This increased adhesion could facilitate stronger binding of the nanoparticles and enhance the negative effects on cell physiology and integrity.

5. Conclusion

In this study, we investigated the combined impact of nanoplastics and elevated temperature on the marine green microalga *Dunaliella tertiolecta*. Our results show that exposure to amine-modified polystyrene nanoplastics (PS-NH_2 NPs) significantly alters the physiology and nanomechanical properties of *D. tertiolecta*, with responses strongly dependent on both nanoplastic concentration and temperature. Increasing concentrations of PS-NH_2 NPs significantly inhibited algal growth, with the effects being more pronounced at elevated temperature (30 °C), as evidenced by reduced specific growth rates and lower EC_{50} values, suggesting a synergistic interaction between nanoplastic toxicity and thermal stress. Increased production of reactive oxygen species (ROS), and biomarkers of oxidative stress, including lipid peroxidation and activities of antioxidant enzymes, confirm that PS-NH_2 NPs disrupt cellular functions at both 18 °C and 30 °C. These biochemical changes were associated with reduced photosynthetic efficiency at both temperatures. Atomic force microscopy (AFM) analysis revealed the adsorption of nanoparticles on the algal surface and temperature-dependent changes in the nanomechanical properties of the cell wall. At 30 °C, the cells showed a significant reduction in stiffness and adhesion, indicating impaired structural integrity, which may affect cell-environment interactions and stress resistance.

Overall, these results suggest that the toxicological effects of PS-NH_2 NPs on microalgae depend on both nanoparticle concentration and temperature. Considering the critical role of marine microalgae as primary producers, this study emphasizes that the combined stressors of nanoplastics and ocean warming pose a significant ecological risk that could disrupt marine food webs and ecosystem productivity. Furthermore, our results emphasize the importance of including multiple environmental variables, including temperature and co-occurring stressors, to improve the ecological risk assessment of nanoplastics under changing ocean conditions.

Funding

This work was supported by the NextGenerationEU (to Mišić Radić, T.)

References

Abassi, S., Wang, H., Ki, J.S., 2020. Molecular cloning of heat shock protein 70 and HOP from the freshwater green algae *Closterium ehrenbergii* and their responses to stress. Cell Stress Chaperon. 25, 1117–1123. https://doi.org/10.1007/s12192-020-01143-8.

Aebi, H., 1984. Catalase in vitro. Methods Enzymol. 105, 121–126. https://doi.org/10.1016/s0076-6879(84)05016-3.

Bellingeri, A., Bergami, E., Grassi, G., Faleri, C., Redondo-Hasselerharm, P., Koelmans, A.A., Corsi, I., 2019. Combined effects of nanoplastics and copper on the freshwater alga *Raphidocelis subcapitata*. Aquat. Toxicol. 210, 179–187. https://doi.org/10.1016/j.aquatox.2019.02.022.

Bergami, E., Pugnalini, S., Vannuccini, M.L., Manfra, L., Faleri, C., Savorelli, F., Dawson, K.A., Corsi, I., 2017. Long-term toxicity of surface-charged polystyrene nanoplastics to marine planktonic species *Dunaliella tertiolecta* and *Artemia franciscana*. Aquat. Toxicol. 189, 159–169. https://doi.org/10.1016/j.aquatox.2017.06.008.

Bhattacharya, P., Lin, S., Turner, J.P., Ke, P.C., 2010. Physical adsorption of charged plastic nanoparticles affects algal photosynthesis. J. Phys. Chem. C, 114, 16556–16561. https://doi.org/10.1021/jp1054759.

Bradford, M.M., 1976. A rapid and sensitive method for the quantitation of microgram quantities of protein utilizing the principle of protein-dye binding. Anal. Biochem. 72, 248-254, https://doi.org/10.1016/0003-2697(76)90527-3.

Capotondi, A., Rodrigues, R.R., Sen Gupta, A., Benthuysen, J.A., Deser, C., Frölicher, T.L., Lovenduski, N.S., Amaya, D.J., Le Grix, N., Xu, T., Hermes, J., Holbrook, N.J., Martinez-Villalobos, C., Masina, S., Roxy, M.K., Schaeffer, A., Schlegel, R.W., Smith, K.E., Wang, C., 2024. A global overview of marine heatwaves in a changing climate. Commun. Earth Environ. 5, e701. https://doi.org/10.1038/s43247-024-01806-9.

Casado, M.P., Macken, A., Byrne, H. J., 2013. Ecotoxicological assessment of silica and polystyrene nanoparticles assessed by a multitrophic test battery, Environ. Int. 51, 97-105. https://doi.org/10.1016/j.envint.2012.11.001.

Chae, Y., Kim, D., Kim, S.W., An, Y.-J., 2018. Trophic transfer and individual impact of nano-sized polystyrene in a four-species freshwater food chain. Sci Rep 8, 284. https://doi.org/10.1038/s41598-017-18849-y.

Cvjetko, P., Milošić, A., Domijan, A.M., Vinković, I.V., Tolić, S., Štefanić, P.P., Letofsky-Papst, I., Tkalec, M., Balen, B., 2017. Toxicity of silver ions and differently coated silver nanoparticles in *Allium cepa* roots. Ecotoxicol. Environ. Saf. 137, 18–28. https://doi.org/10.1016/j.ecoenv.2016.11.009.

European Commission, 2018. A European Strategy for Plastics in a Circular Economy. Communication from the Commission to the European Parliament, the Council, the European Economic and Social Committee and the Committee of the Regions. Brussels, January 16th 2018 COM (2018). Available online: https://eur-lex.europa.eu/legal-content/EN/TXT/PDF/?uri=CELEX:52018DC0028 (assessed Jul 01 2025).

Fox-Kemper, B., Hewitt, H.T., Xiao, C., 2021. Ocean, cryosphere and sea level change, in: Masson- Delmotte, V. (Ed.), Climate Change 2021: The physical science basis. Contribution of working group I to the sixth assessment report of the intergovernmental panel on climate

change, Cambridge, University Press, pp. 1211–1362. https://doi.org/10.1017/9781009157896.011.

Gomes, T., Almeida, A.C., Georgantzopoulou, A., 2020. Characterization of cell responses in Rhodomonas baltica exposed to PMMA nanoplastics. Sci. Total Environ. 726, 138547. https://doi.org/10.1016/j.scitotenv.2020.138547.

Gonçalves, J.M., Bebianno, M.J., 2021. Nanoplastics impact on marine biota: A review. Environ. Pollut. 273, 116426. https://doi.org/10.1016/j.envpol.2021.116426.

González-Fernández, C., Le Grand, F., Bideau, A., Huvet, A., Paul-Pont, I., Soudant, P., 2020. Nanoplastics exposure modulate lipid and pigment compositions in diatoms. Environ. Pollut. 262, 114274. https://doi.org/10.1016/j.envpol.2020.114274.

Guillard, R.R.L., 1975. Culture of phytoplankton for feeding marine invertebrates, in: Smith, W.L., Chanley, M.H. (Eds.), Culture of marine invertebrate animals - Proceedings of the 1st conference on culture of marine invertebrate animals greenport. Springer, Boston, pp. 29–60. http://dx.doi.org/10.1007/978-1-4615-8714-9_3.

Hanachi, P., Khoshnamvand, M., Walker, T.R., Hamidian, A.H., 2022. Nano-sized polystyrene plastics toxicity to microalgae *Chlorella vulgaris*: Toxicity mitigation using humic acid. Aquat. Toxicol. 245, 106123. https://doi.org/10.1016/j.aquatox.2022.106123.

Hazeem, L.J., Yesilay, G., Bououdina, M., Perna, S., Cetin, D., Suludere, Z., Barras, A., Boukherroub, R., 2020. Investigation of the toxic effects of different polystyrene micro-and nanoplastics on microalgae *Chlorella vulgaris* by analysis of cell viability, pigment content, oxidative stress and ultrastructural changes. Mar. Pollut. Bull. 156, e111278. https://doi.org/10.1016/j.marpolbul.2020.111278.

Heath, R.L., Packer, L., 1968. Photoperoxidation in isolated chloroplasts. I. Kinetics and stoichiometry of fatty acid peroxidation. Arch. Biochem. Biophys. 125, 189–198. https://doi.org/10.1016/0003-9861(68)90654-1.

Hertz, H., 1882. Über die Berührung fester elastischer Körper. J. Reine Angew Math 92, 156–171. https://doi.org/10.1515/crll.1882.92.156.

Hong, Y., Hu, H.Y., Xie, X., Sakoda, A., Sagehashi, M., Li, F., 2009. Gramine-induced growth inhibition, oxidative damage and antioxidant responses in freshwater cyanobacterium *Microcystis aeruginosa*. Aquat. Toxicol. 91, 262–269. https://doi.org/10.1016/j.aquatox.2008.11.014.

Hou, X., Hu, X., Mu, L., Wei, Y., 2025. Heatwaves increase the polystyrene nanoplastic-induced toxicity to marine diatoms through interfacial interaction regulation. J. Haz. Mat. 483, 136703. https://doi.org/10.1016/j.jhazmat.2024.136703.

Hu, X., Tang, X., Bi, Z., Zhao, Q., Ren, L., 2021. Adaptive evolution of microalgae *Schizochytrium* sp. under high temperature for efficient production of docosahexaeonic acid. Algal Res. 54, 102212. https://doi.org/10.1016/j.algal.2021.102212.

Jalaudin Basha, N.N., Adzuan Hafiz, N.B., Osman, M.S., Abu Bakar, N.F., 2023. Unveiling the noxious effect of polystyrene microplastics in aquatic ecosystems and their toxicological behavior on fishes and microalgae. Front. Toxicol. 5, 1135081. https://doi.org/10.3389/ftox.2023.1135081.

Jambeck, J., Geyer, R., Wilcox, C., Siegler, T.R., Perryman, M., Andrady, A., Narayan, R., Law, K.L., 2015. Plastic waste inputs from land into the ocean. Science 347, 768–771. https://doi.org/10.1126/science.1260352.

Jolly, E.R., 2018. HSP70, HSP90A, and HSP90B are differentially regulated in response to thermal, osmotic and hypoxic stressors. Ann. Experiment. Mol. Biol. 1, 1–9. https://doi.org/10.23880/aemb-16000101.

Khoshnamvand, M., Hamidian, A.H., Ashtiani, S., Ali, J., Pei, D.-S., 2024. Combined toxic effects of polystyrene nanoplastics and lead on *Chlorella vulgaris* growth, membrane lipid peroxidation, antioxidant capacity, and morphological alterations. Environ. Sci. Pollut. Res. 31, 28620–28631. https://doi.org/10.1007/s11356-024-33084-5.

Khoshnamvand, M., Hanachi, P., Ashtiani, S., Walker, T. R., 2021. Toxic effects of polystyrene nanoplastics on microalgae *Chlorella vulgaris*: Changes in biomass, photosynthetic pigments and morphology. Chemosphere 280, e130725. https://doi.org/10.1016/j.chemosphere.2021.130725.

Kumari, S., Satapathy, S., Datta, M., Kumar, S., 2022. Adaptation of microalgae to temperature and light stress, in: Roy, S., Mathur, P., Chakraborty, A.P., Saha, S.P. (Eds.), Plant stress: Challenges and management in the new decade, Advances in Science, Technology & Innovation. Springer International Publishing, Cham, pp. 123–134. https://doi.org/10.1007/978-3-030-95365-2_8.

Li, L., Liu, Q., Li, B., Zhao, Y., 2024. The effecting mechanisms of 100 nm sized polystyrene nanoplastics on the typical coastal *Alexandrium tamarense*. Int. J. Mol. Sci. 25, 7297. https://doi.org/10.3390/ijms25137297.

Li, X., Wang, Z., Chen, Y., Li, Q., 2024. Polystyrene microplastics induce photosynthetic impairment in *Navicula* sp. at physiological and transcriptomic levels. Int. J. Mol. Sci. 26, 148. https://doi.org/10.3390/ijms26010148.

López Muñoz, I., Bernard, O., 2021. Modeling the influence of temperature, light Intensity and oxygen concentration on microalgal growth rate. Processes 9, 496. https://doi.org/10.3390/pr9030496.

Mišić Radić, T., Vukosav, P., Komazec, B., Formosa-Dague, C., Domazet Jurašin, D., Peharec Štefanić, P., Čačković, A., Juraić, K., Ivošević DeNardis, N., 2022. Nanoplastic-induced nanostructural, manomechanical, and antioxidant response of marine diatom *Cylindrotheca closterium*. Water 14, 2163. https://doi.org/10.3390/w14142163.

Nakano, Y., Asada, K., 1981. Hydrogen peroxide is scavenged by ascorbate-specific peroxidase in spinach chloroplasts. Plant Cell Physiol. 22, 867–880. https://doi.org/10.1093/oxfordjournals.pcp.a076232.

Nolte, T.M., Hartmann, N.B., Kleijn, J.M., Garnæs, J., van de Meent, D., Hendriks, A.J., Baun, A., 2017. The toxicity of plastic nanoparticles to green algae as influenced by surface modification, medium hardness and cellular adsorption. Aquat. Toxicol. 183, 11–20. https://doi.org/10.1016/j.aquatox.2016.12.005.

Novosel, N., Mišić Radić, T., Levak Zorinc, M., Zemla, J., Lekka, M., Vrana, I., Gašparović, B., Horvat, L., Kasum, D., Legović, T., Žutinić, P., Gligora Udovič, M., Ivošević deNardis, N., 2022a. Salinity-induced chemical, mechanical, and behavioral changes in marine microalgae. J. Appl. Phycol. 34, 1293–1309. https://doi.org/10.1007/s10811-022-02734-x.

Novosel, N., Mišić Radić, T., Zemla, J., Lekka, M., Čačković, A., Kasum, D., Legović, T., Žutinić, P., Gligora Udovič, M., Ivošević DeNardis, N., 2022b. Temperature-induced response in algal cell surface properties and behaviour: An experimental approach. J. Appl. Phycol. 34, 243–259. https://doi.org/10.1007/s10811-021-02591-0.

OECD Test No. 201., 2011. Organisation for Economic Cooperation and Development. Freshwater algae and cyanobacteria, growth inhibition test. In OECD Guidelines for the Testing of Chemicals, Section 2. Effects on Biotic Systems; Organisation for Economic Cooperation and Development: Paris, France.

Piccardo, M., Renzi, M., Terlizzi, A., 2020. Nanoplastics in the oceans: Theory, experimental evidence and real world. Mar. Pollut. Bullet. 157, 111317. https://doi.org/10.1016/j.marpolbul.2020.111317.

Pillet, F., Dague, E., Pečar Ilić, J., Ružić, I., Rols, M.-P., Ivošević DeNardis, N., 2019. Changes in nanomechanical properties and adhesion dynamics of algal cells during their growth. Bioelectrochemistry 127, 154–162. https://doi.org/10.1016/j.bioelechem.2019.02.011.

Rimet, F., 2012. Recent views on river pollution and diatoms. Hydrobiologia 683, 1–24. https://doi.org/10.1007/s10750-011-0949-0.

Sader, J.E., Larson, I., Mulvaney, P., White, L.R., 1995. Method for the calibration of atomic force microscope cantilevers. Rev. Sci. Instrum. 66, 3789–3798. https://doi.org/10.1063/1.1145439.

Sendra, M., Staffieri, E., Yeste, P.M., Moreno-Garrido, I., Gatica, J.M., Corsi, I., Julián Blasco, J., 2019. Are the primary characteristics of polystyrene nanoplastics responsible for toxicity and ad/absorption in the marine diatom *Phaeodactylum tricornutum*? Environ. Pollut. 249, 610–619. https://doi.org/10.1016/j.envpol.2019.03.047.

Sjollema, S.B., Redondo-Hasselerharm, P., Leslie, H.A., Kraak, M.H.S., Vethaak, A.D., 2016. Do plastic particles affect microalgal photosynthesis and growth? Aquat. Toxicol. 170, 259–261. https://doi.org/10.1016/j.aquatox.2015.12.002.

Tudesque, L., Grenouillet, G., Gevrey, M., Khazraie, K., Brosse, S., 2012. Influence of small-scale gold mining on French Guiana streams: Are diatom assemblages valid disturbance sensors? Ecol. Indic. 14, 100–106. https://doi.org/10.1016/J.ECOLIND.2011.07.018.

Wang, F., Guan, W., Xu, L., Ding, Z., Ma, H., Ma, A., Terry, N., 2019. Effects of nanoparticles on algae: adsorption, distribution, ecotoxicity and fate. Appl. Sci. 9, 1534. https://doi.org/10.3390/app9081534.

Wang, S., Liu, M., Wang, J., Huang, J., Wang, J., 2020. Polystyrene nanoplastics cause growth inhibition, morphological damage and physiological disturbance in the marine microalga *Platymonas helgolandica*. Mar. Pollut. Bullet., 158, 111403. https://doi.org/10.1016/j.marpolbul.2020.111403.

Zaki, M.R.M., Aris, A.Z., 2022. An overview of the effects of nanoplastics on marine organisms. Sci. Total Environ. 831, 154757. https://doi.org/10.1016/J.SCITOTENV.2022.154757.

Zhao, T., Tan, L., Zhu, X., Huang, W. Wang, J., 2020. Size-dependent oxidative stress effect of nano/micro-scaled polystyrene on *Karenia mikimotoi*. Mar. Pollut. Bull. 154, 111074. https://doi.org/10.1016/j.marpolbul.2020.111074.

Zhu, H., Fu, S., Zou, H., Su, Y., Zhang, Y., 2021. Effects of nanoplastics on microalgae and their trophic transfer along the food chain: recent advances and perspectives. Environ. Sci.: Processes Impacts 23, 1873–1883. https://doi.org/10.1039/D1EM00438G.

TABLES

Table 1. Average hydrodynamic diameter (d_h) obtained from the volume size distributions and zeta potential (ζ), with standard deviations, of PS-NH_2 nanoparticles (50 μg mL^{-1}) at two temperatures (18 °C and 30 °C) in ultrapure water (UPW) and filtered natural seawater (FSW) obtained by dynamic (DLS) and electrophoretic light scattering (ELS).

Temperature / °C	Time / days	d_h / nm (vol. %)		ζ / mV	
		UPW	FSW	UPW	FSW
18	1	47.4 ± 2.3 (100 %)	54.4 ± 1.1 (98.1 ± 0.6%)	39.3 ± 0.9	9.6 ± 1.8
	5	48.4 ± 2.1 (100 %)	57.4 ± 1.2 (97.7 ± 1.3%)	36.5 ± 9.7	7.7 ± 2.0
30	1	50.6 ± 0.9 (100 %)	58.2 ± 0.9 (96.8 ± 0.7%)	35.8 ± 1.9	9.9 ± 0.9
	5	50.4 ± 0.7 (100 %)	62.1 ± 0.7 (95.4 ± 2.7%)	38.2 ± 3.2	7.7 ± 0.6

FIGURE CAPTIONS

Fig. 1. TEM images of PS-NH_2 nanoparticles (50 µg mL^{-1}) at two temperatures (18 °C and 30 °C) in ultrapure water (UPW) and filtered natural seawater (FSW). PS-NH_2 nanoparticles in UPW immediately after mixing (18 °C, day 0) (A), after 24 h (18 °C, day 1) (B), after 120 h (18 °C, day 5) (C), after 24 h (30 °C, day 1) (D) and after 120 h (30 °C, day 5) (E). PS-NH_2 nanoparticles in FSW immediately after mixing (18 °C, day 0) (F), after 24 h (18 °C, day 1) (G), after 120 h (18 °C, day 5) (H), after 24 h (30 °C, day 1) (I) and after 120 h (30 °C, day 5) (J).

Fig. 2. Growth curves of *D. tertiolecta* exposed to PS-NH_2 nanoparticles (0–3 µg mL^{-1}) at a temperature of 18 °C (A) and 30 °C (B), measured by cell density over a period of 5 days. Mean values of triplicate determinations with standard deviations are shown.

Fig. 3. Levels of reactive oxygen species (ROS) in *D. tertiolecta* after 5-day exposure to PS-NH_2 nanoparticles at concentrations of 1.0, 1.5 and 2.0 µg mL^{-1} at 18 °C and 30 °C. The graphs show: the amount of superoxide radicals determined using the dihydroethidium (DHE) probe (A) and the total intracellular ROS levels measured with the 2',7'-dichlorodihydrofluorescein diacetate (H_2DCFDA) probe (B). Data are presented as boxplots showing the median, interquartile range (Q3-Q1) and whiskers. Statistically significant differences between treatments within the same temperature are indicated by different lowercase letters (Neuman-Keuls test, $p < 0.05$).

Fig. 4. Specific activities of the antioxidant enzymes: pyrogallol peroxidase, PPX (A), ascorbate peroxidase, APX (B), and catalase, CAT (C) in *D. tertiolecta* after 5-day exposure to PS-NH_2 nanoparticles at concentrations of 1.0, 1.5 and 2.0 µg mL^{-1} at 18 °C and 30 °C. Data are presented as boxplots showing the median, interquartile range (Q3-Q1) and whiskers. Statistically significant differences between treatments within the same temperature are indicated by different lowercase letters (Neuman-Keuls test, $p < 0.05$), while differences between the same treatments at different temperatures are marked by an asterisk (*) placed above the corresponding bar at 30 °C (t-test, $p < 0.05$).

Fig. 5. Lipid peroxidation expressed as malondialdehyde (MDA) concentration in *D. tertiolecta* after 5 days of exposure to PS-NH_2 nanoparticles at concentrations of 1.0, 1.5 and 2.0 µg mL^{-1} at 18 °C and 30 °C. Data are presented as boxplots showing the median, interquartile range (Q3-Q1) and whiskers. Statistically significant differences between treatments within the same temperature are indicated by different lowercase letters (Neuman-Keuls test, $p < 0.05$), while differences between the same treatments at different temperatures are marked with an asterisk (*) placed above the corresponding bar at 30 °C (t-test, $p < 0.05$).

Fig. 6. Analysis of the maximum quantum yield of photosystem II (F_v/F_m) (A) and the performance index of light absorption efficiency (PI_{abs}) (B) in *D. tertiolecta* after 5-day exposure to PS-NH_2 nanoparticles at concentrations of 1.0, 1.5 and 2.0 µg mL^{-1} at 18 °C and 30 °C. The data are presented as boxplots showing the median, interquartile range (Q3-Q1) and whiskers. Statistically significant differences between treatments within the same temperature are indicated by different lowercase letters (Neuman-Keuls test, $p < 0.05$), while differences between the same treatments at different temperatures are marked with an asterisk (*) placed above the corresponding bar at 30 °C (t-test, $p < 0.05$).

Fig. 7. AFM images of *D. tertiolecta* cells from: a control culture grown at 18 ºC (A, B), a culture exposed to 2.0 µg mL^{-1} PS-NH_2 nanoparticles and grown at 18 ºC (C, D), a control culture grown at 30 ºC (E, F) and a culture exposed to 2.0 µg mL^{-1} PS-NH_2 nanoparticles and grown at 30 ºC (G, H). The AFM images are presented as deflection images (A, C, E, G) and height images (B, D, F, H) with insets showing corresponding deflection images of the same area and vertical profiles along the indicated lines. The images are acquired using contact mode in air, with scan sizes: 15 µm x 15 µm (A, C, E, G) and 3 µm x 3 µm (B, D, F, H and corresponding insets) with a vertical scale of 1.0 µm (B), 500 nm (D), 1.5 µm (F) and 400 nm (H).

Fig. 8. Nanomechanical properties of *D. tertiolecta* grown at 18 °C and 30 °C and exposed to PS-NH_2 nanoparticles (2.0 µg mL^{-1} PS-NH_2). Optical micrographs of *D. tertiolecta* cells and AFM MLCT-Bio D cantilever (A). An example of the force curve recorded on a single *D. tertiolecta* cell (B). Young's modulus of *D. tertiolecta* cultured at 18 °C and 30 °C and exposed to PS-NH_2 nanoparticles (2.0 µg mL^{-1} PS-NH_2) (C). Adhesion of *D. tertiolecta* cultured at 18 °C and 30 °C and exposed to PS-NH_2 nanoparticles (2.0 µg mL^{-1} PS-NH_2) (D). A box with whiskers represents the median ± interquartile range (Q3-Q1). Statistical significance was obtained from Kruskal-Wallis test and post-hoc Dunn test at the 0.05, 0.01, 0.001 level (* $p < 0.05$, ** $p < 0.01$, *** $p < 0.001$, ns – not statistically significant).

Figure(s)

Click here to access/download;Figure(s);Figure_1.tif

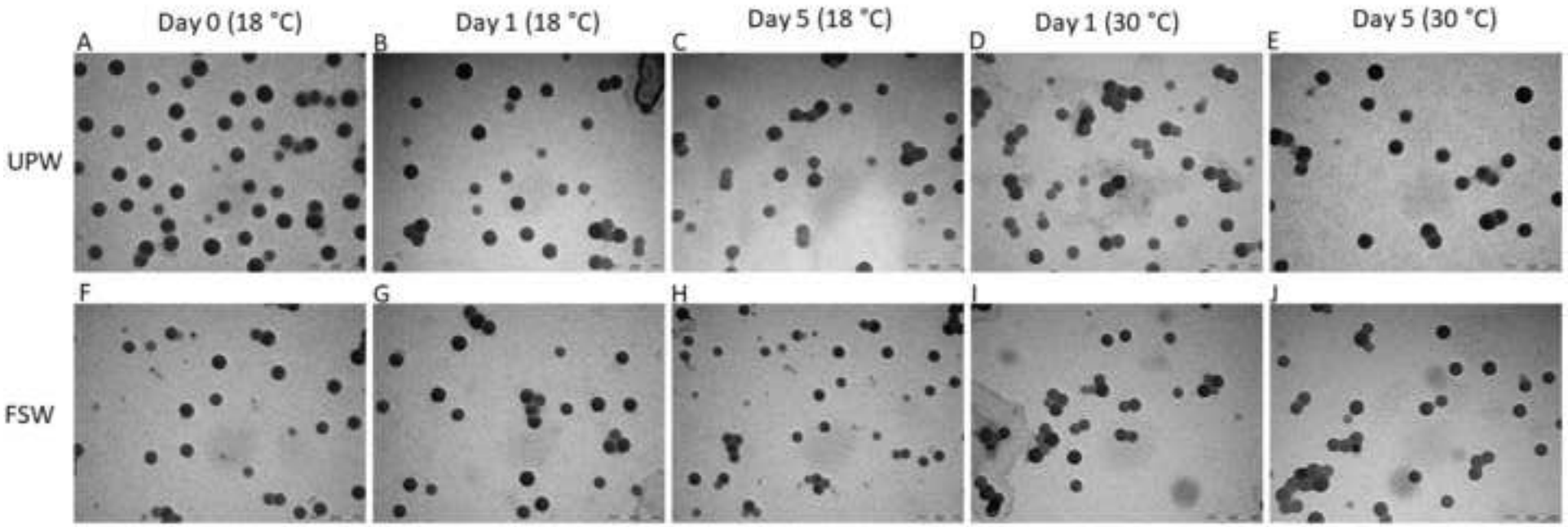

Figure(s)

Click here to access/download;Figure(s);Figure_2.tiff

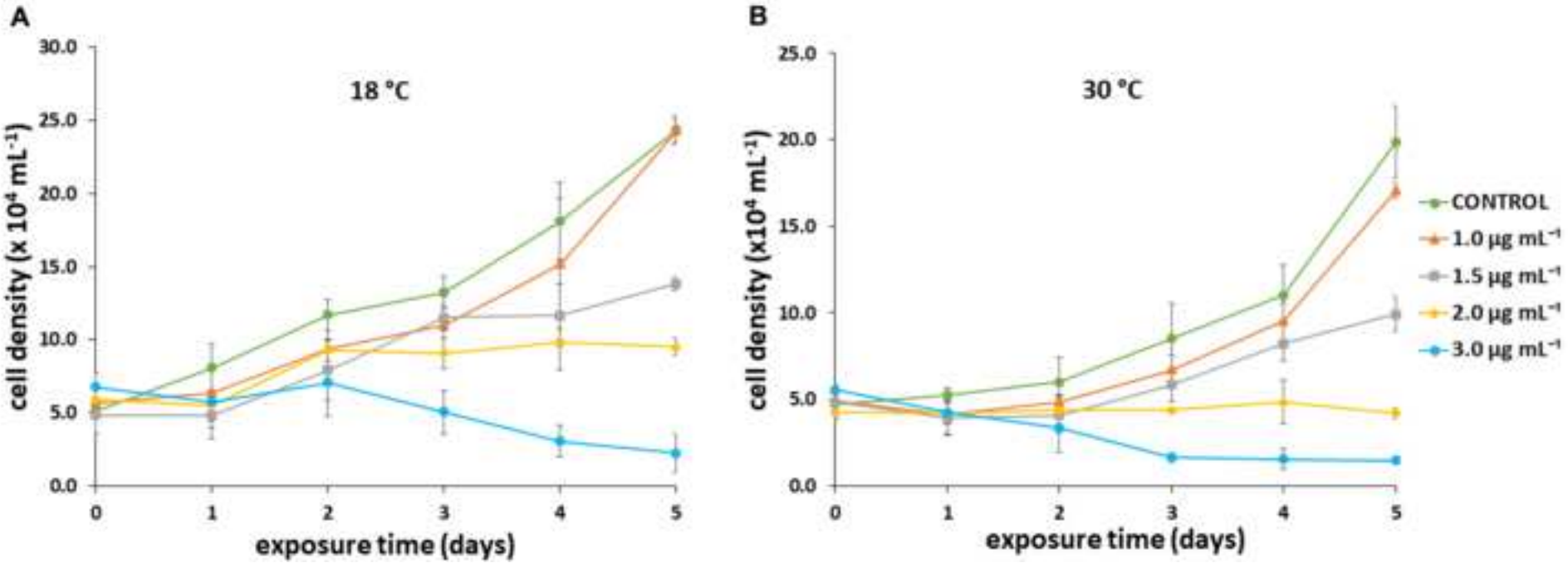

Figure(s)

Click here to access/download;Figure(s);Figure_3.tif

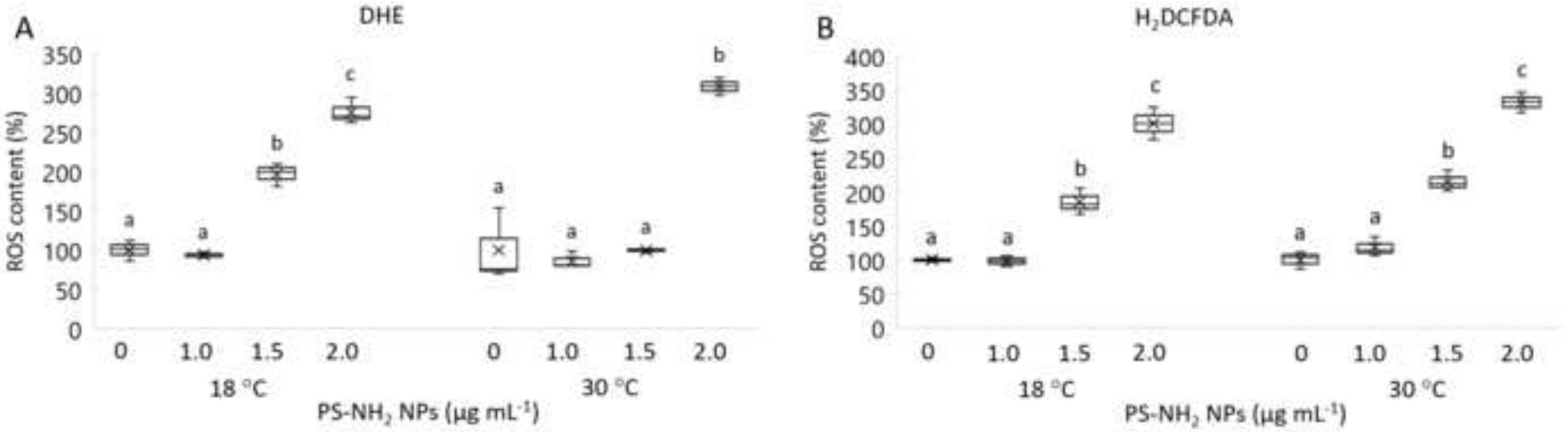

Figure(s)

Click here to access/download;Figure(s);Figure_4.tif

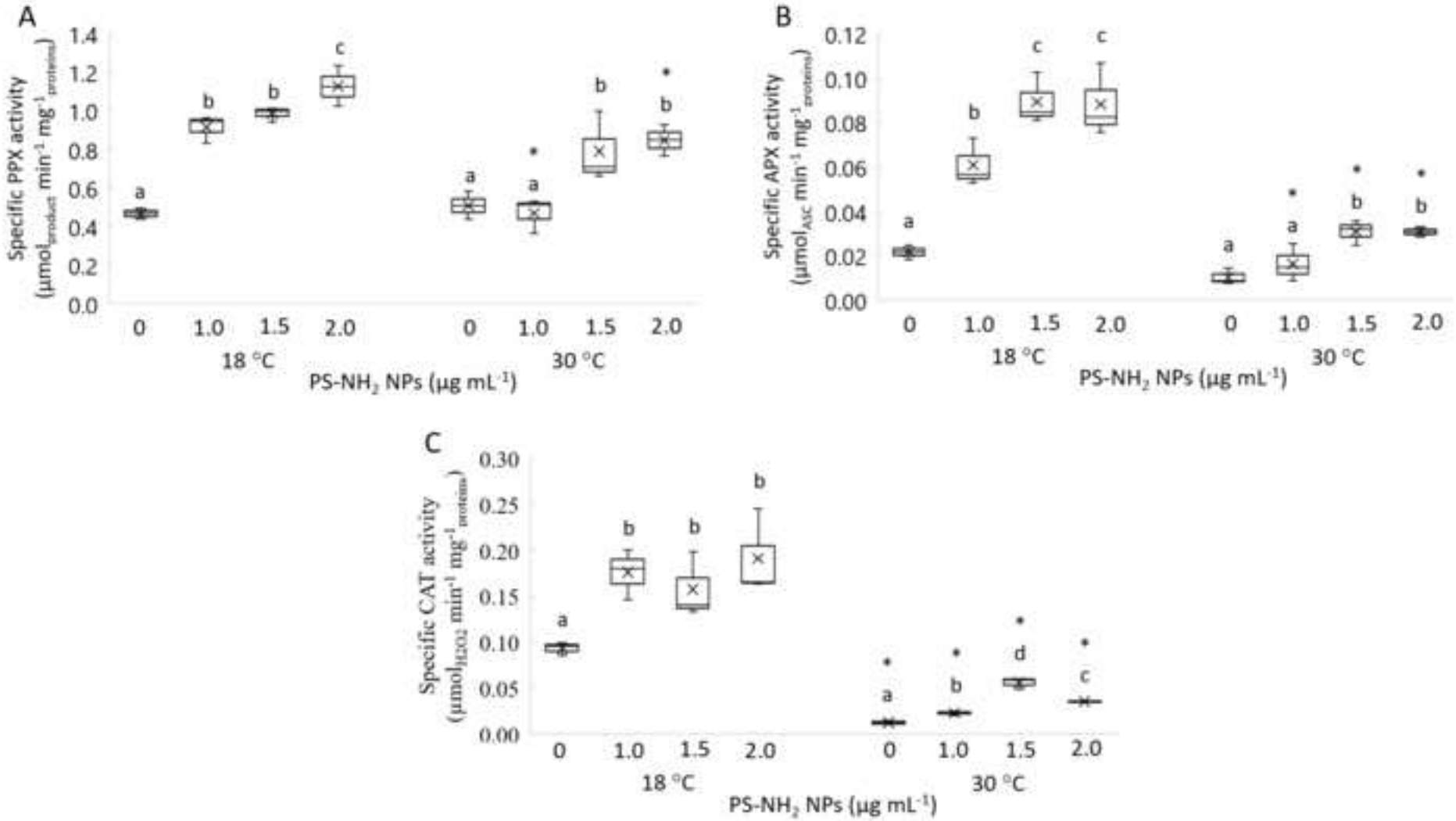

Figure(s)

Click here to access/download;Figure(s);Figure_5.tif

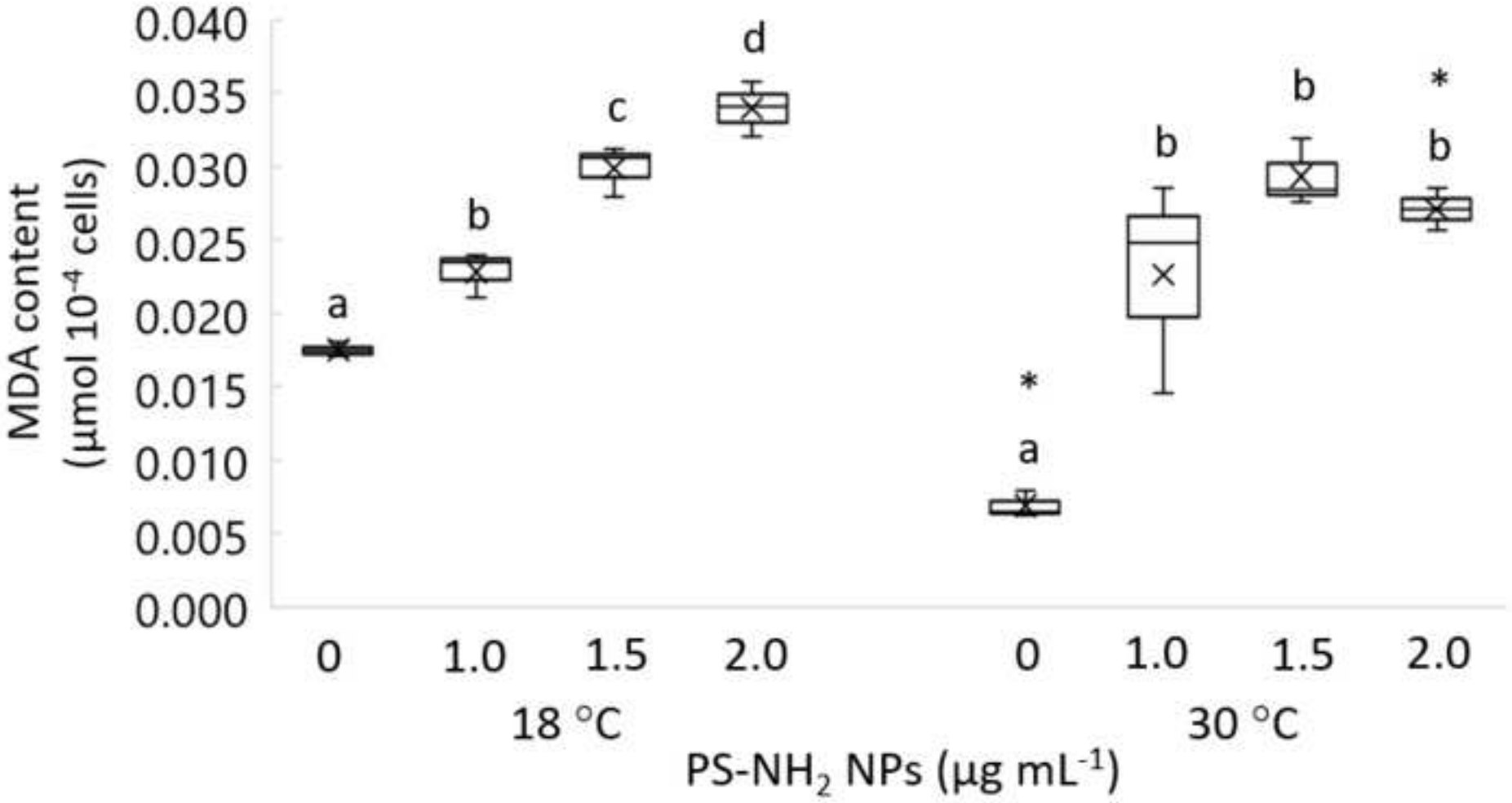

Figure(s)

Click here to access/download;Figure(s);Figure_6.tif

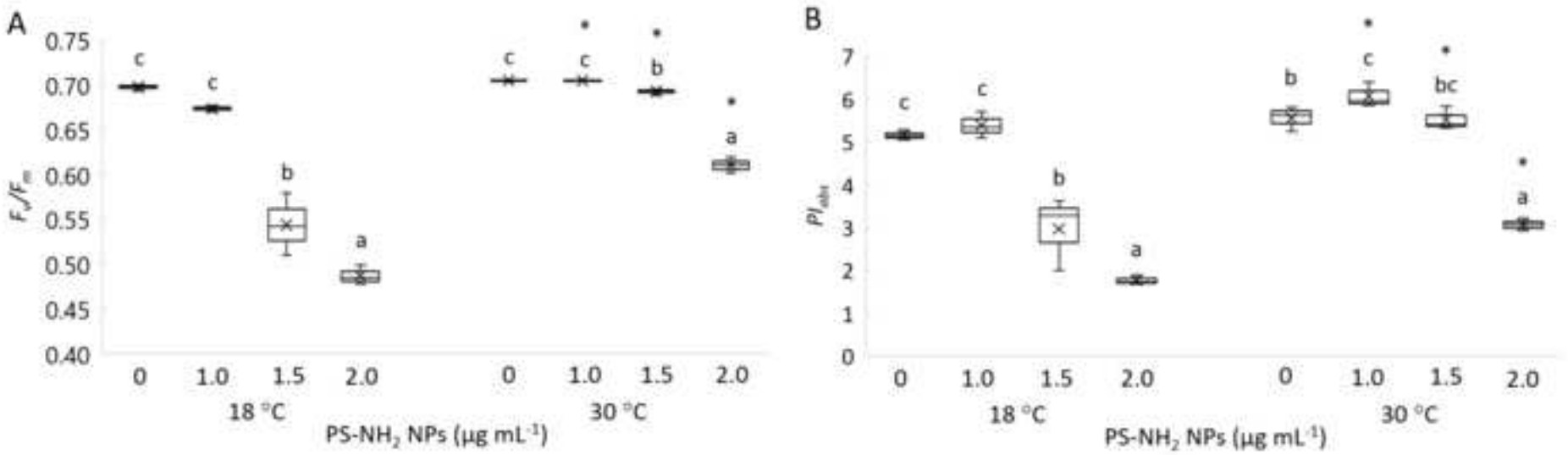

Figure(s)

Click here to access/download;Figure(s);Figure_7.tiff

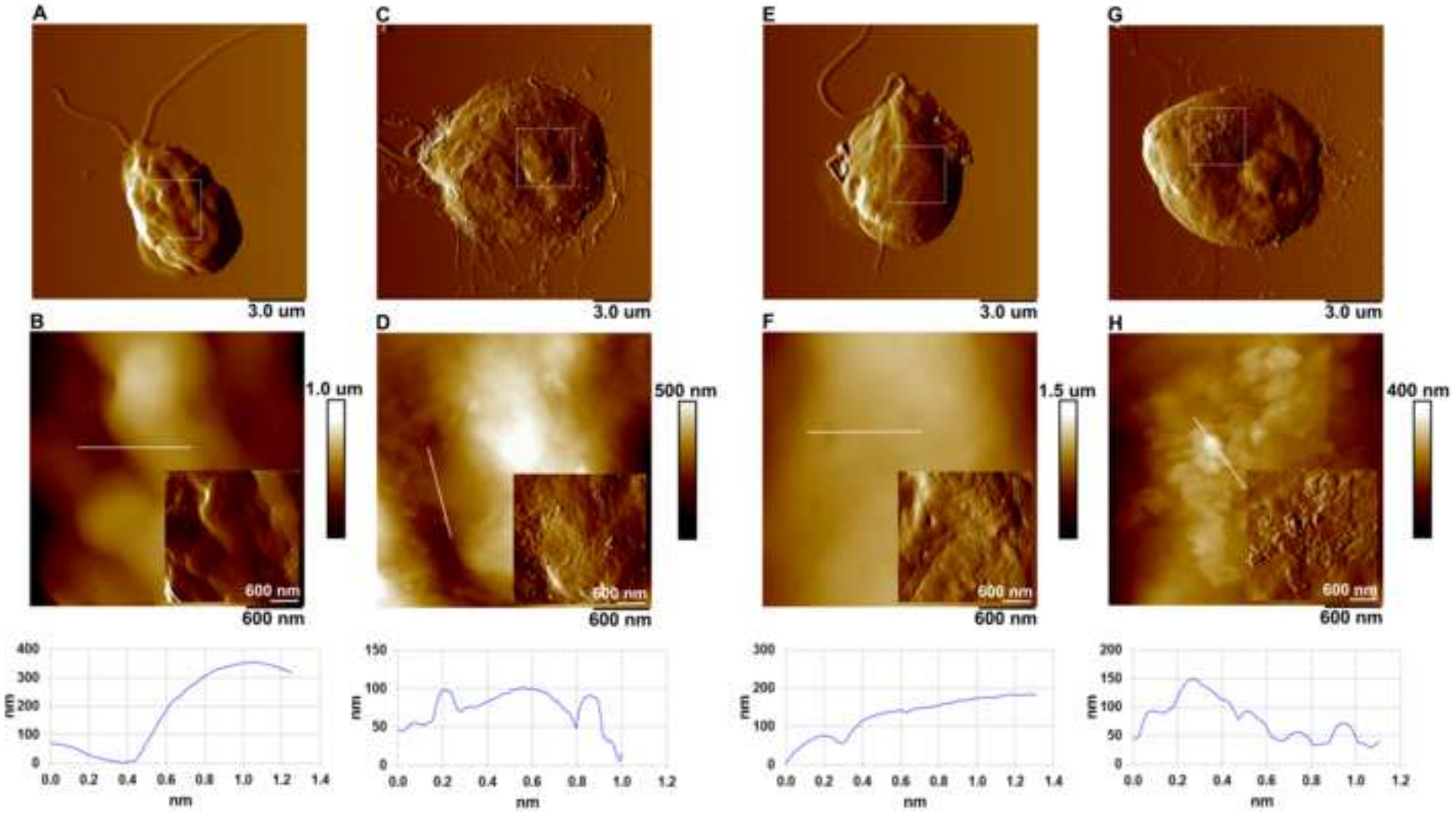

Figure(s)

Click here to access/download;Figure(s);Figure_8.tif

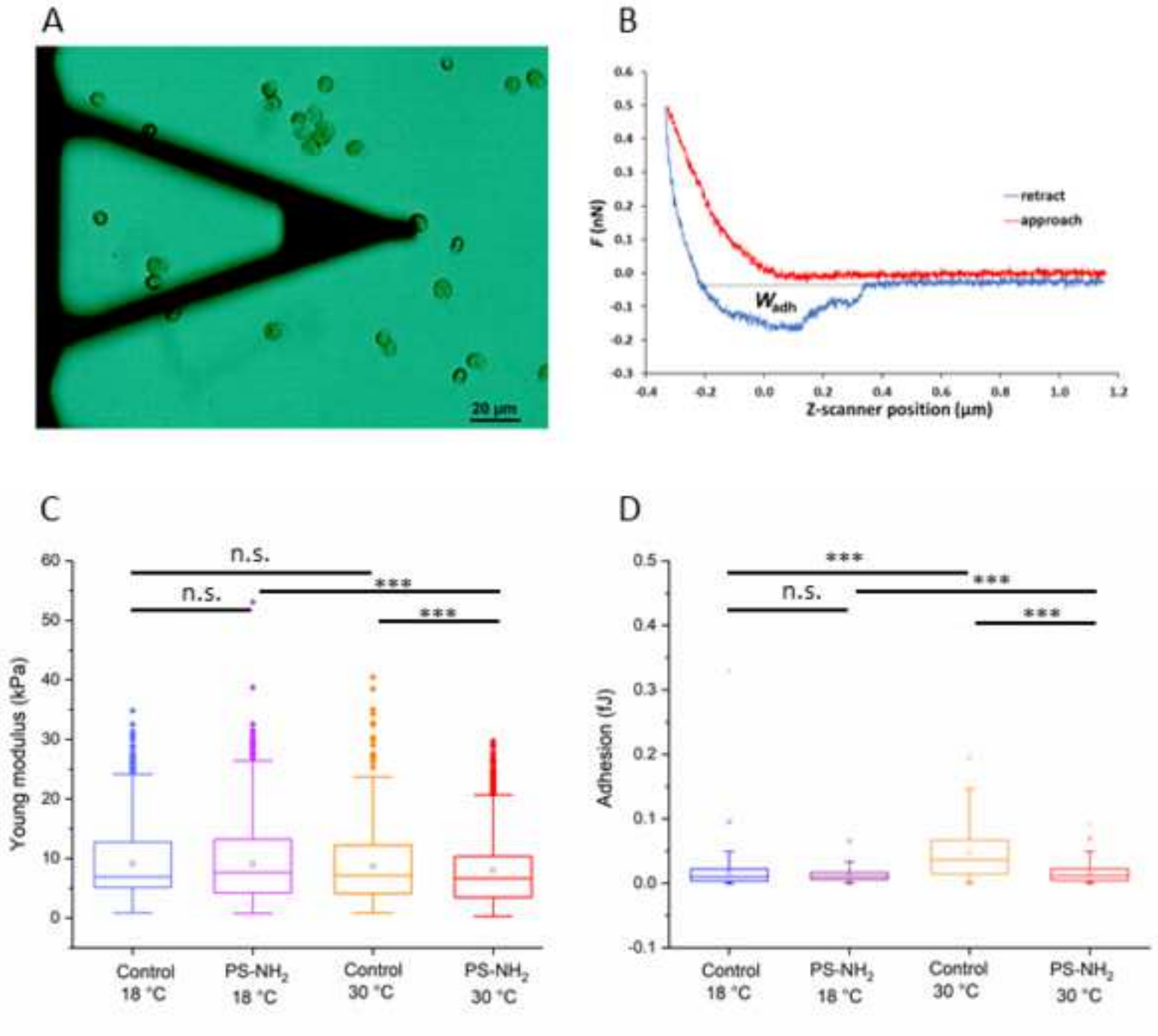

Declaration of interests

☒The authors declare that they have no known competing financial interests or personal relationships that could have appeared to influence the work reported in this paper.

☐The authors declare the following financial interests/personal relationships which may be considered as potential competing interests: